Electronic Supplementary Material (ESI) for Materials Chemistry Frontiers.
This journal is © the Partner Organisations 2018

Liquid crystal gelators with photo-responsive and AIE properties

Xia Yu,[a,†] Hui Chen,[b,†] Xiang Shi,[c] Pierre-Antoine Albouy,[c] Jia Guo,[a] Jun Hu*[a] and Min-Hui Li*[a,b]

[a]*Beijing Advanced Innovation Center for Soft Matter Science and Engineering, Beijing University of Chemical Technology, Beijing 100029, China. Email: min-hui.li@chimieparistech.psl.eu; jhu@mail.buct.edu.cn*

[b]*Chimie ParisTech, PSL University Paris, CNRS, Institut de Recherche de Chimie Paris, 75005 Paris, France. Email: min-hui.li@chimieparistech.psl.eu*

[c]*Université Paris-Sud, CNRS, Laboratoire de Physique des Solides, UMR8502, 91405 Orsay Cedex, France.*

[†]These authors contributed equally to this work.

Contents

1. Synthesis of *trans*-C$_n$-Chol **S2**

2. Liquid crystal behavior **S3**

3. Gelation **S7**

3.1 Gel ability **S7**

3.2 Morphologies **S8**

3.3 Supramolecular chirality **S8**

3.4 Driving force of gelation **S9**

4. AIE characteristics **S10**

5. Photo-responsiveness **S11**

6. MS, ^{1}H and ^{13}C NMR spectra **S12**

1. Synthesis of *trans*-C_n-chol

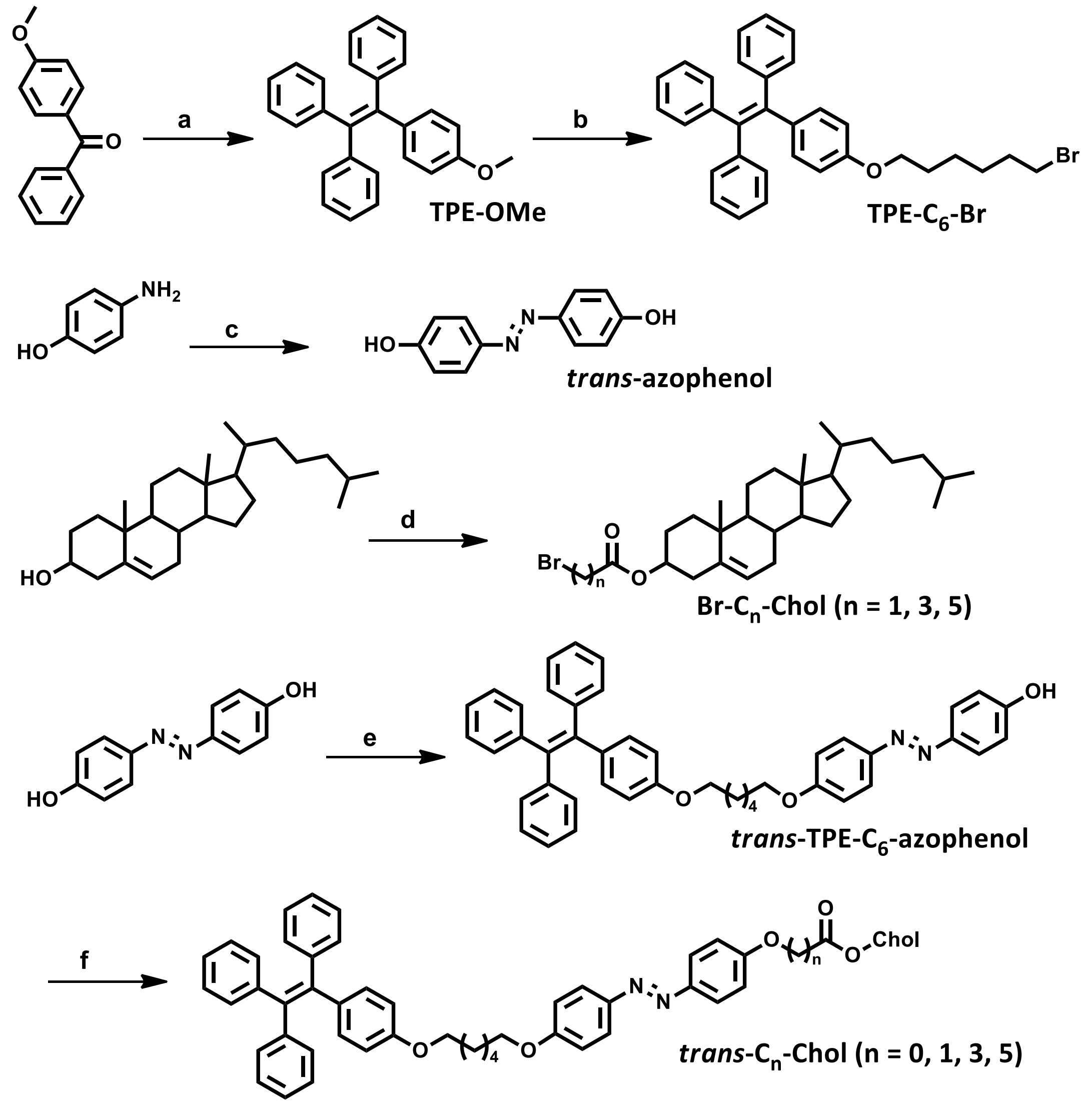

Scheme S1. Synthetic route of ***trans*-C_n-Chol.** Reaction conditions: a) i. n-butyllithium, 0 °C, 0.5 h, diphenylmethane, THF, rt, 6 h; ii. PTSA, toluene, 120 °C, 12 h; b) i. BBr_3, -20 °C, 4 h; ii. 1,6-dibromohexane, K_2CO_3, MeCN, 50 °C, 24 h; c) i. HCl, $NaNO_2$, methanol/H_2O, 0 °C, 0.5 h; ii. phenol, KOH, H_2O, rt, 24 h; d) Br-C_n-CO_2H (n = 1, 3, 5), EDCI, DMAP, DCM, rt, 12h; e) TPE-C_6-Br, K_2CO_3, MeCN, 85 °C, 24 h; f) R-C_n-Chol (R = Cl, n = 0; R = Br, n = 1, 3, 5), K_2CO_3, DMF, 50 °C, 24 h.

2. Liquid crystal behaviour

Table S1. Phase transition temperatures (°C) and enthalpies (kJ mol^{-1}, in brackets) of *trans*-C_n-Chol upon first heating and first cooling cycle at a rate of 2 °C min^{-1}.

compounds		re-organization	Cr-Iso	SmA-LC2	Cr-SmA	SmA-Iso
trans-C_0-Chol	Heating	161.1 (1.4)	-	-	175.1 (46.0)	178.3 (5.9)
	Cooling	-	-	-	-	171.5 (4.0)
trans-C_1-Chol	Heating	-	164.2 (76.8)	-	-	-
	Cooling	-	-	-	-	154.6 (13.8)
trans-C_3-Chol	Heating	-	-	-	161.7 (38.3)	164.7 (0.7)
	Cooling	-	-	-	-	160.1 (11.7)
trans-C_5-Chol	Heating	146.2 (11.1)	171.5 (65.6)	-	-	-
	Cooling	-	-	139.1 (36.7)	-	155.9 (14.9)

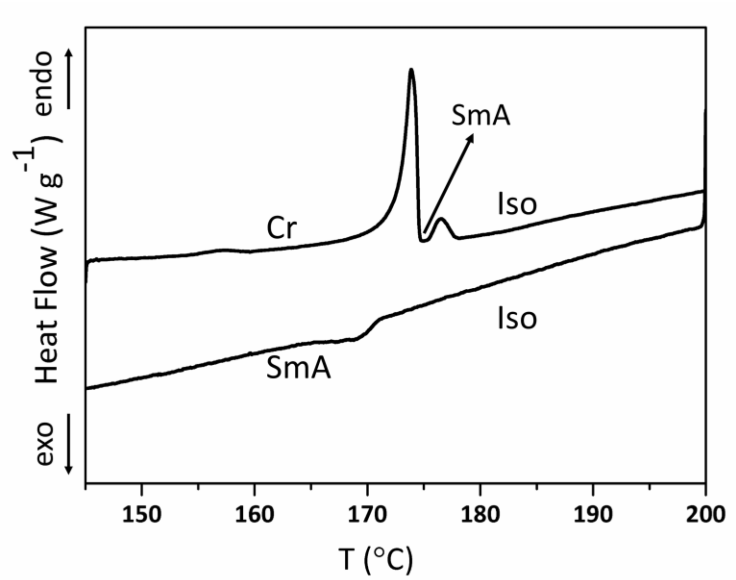

Fig. S1 DSC thermogram of *trans*-C_0-Chol at first heating and cooling (0.5 °C min^{-1}).

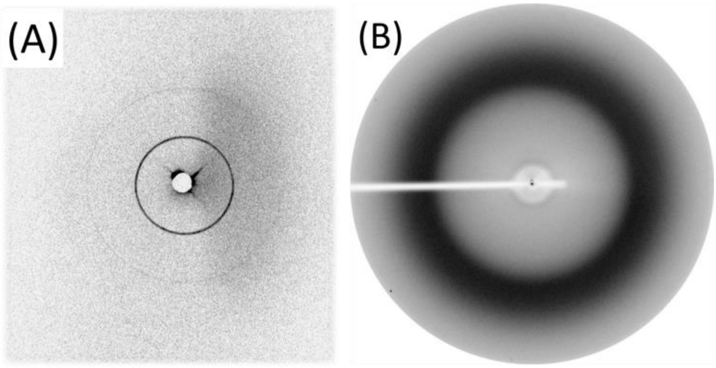

Fig. S2 SAXS (A) and WAXS (B) of *trans*-C_0-Chol.

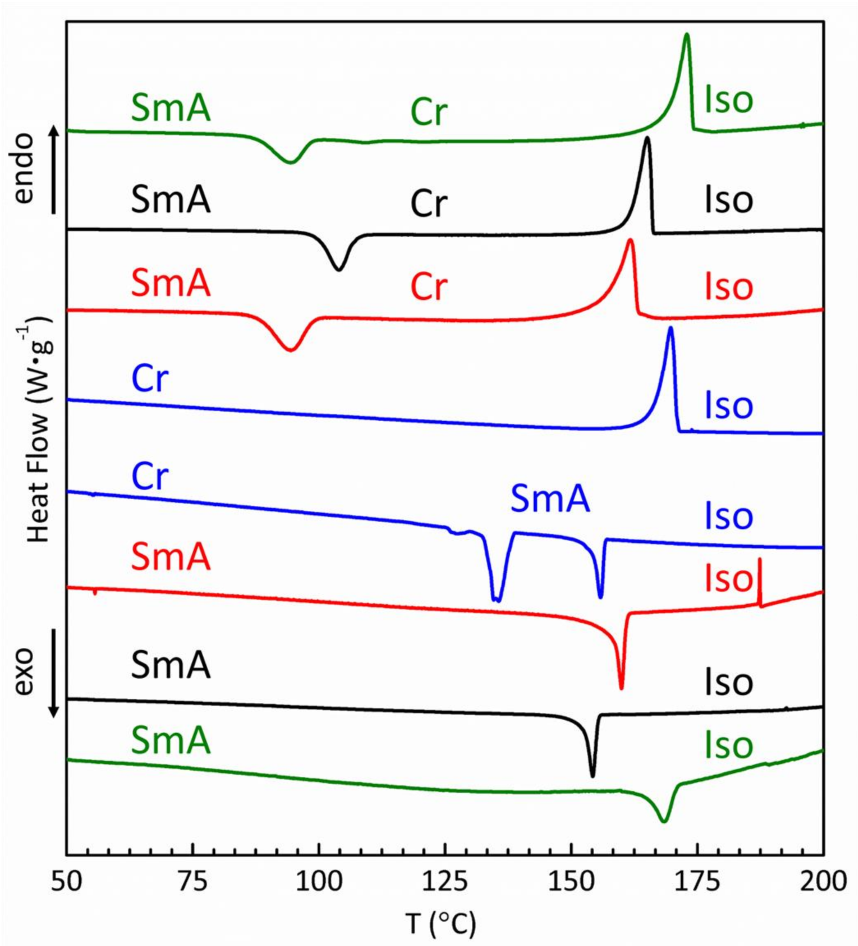

Fig. S3 DSC thermograms of *trans*-C_0-Chol (green lines), *trans*-C_1-Chol (black lines), *trans*-C_3-Chol (red lines) and *trans*-C_5-Chol (blue lines) upon the second heating (4 upper curves) and second cooling (4 lower curves) cycle at a rate of 2 °C min^{-1}. Three samples, *trans*-C_0-Chol, *trans*-C_1-Chol and *trans*-C_3-Chol, exhibited hot-recrystallization upon the second and further heating at around 100 °C.

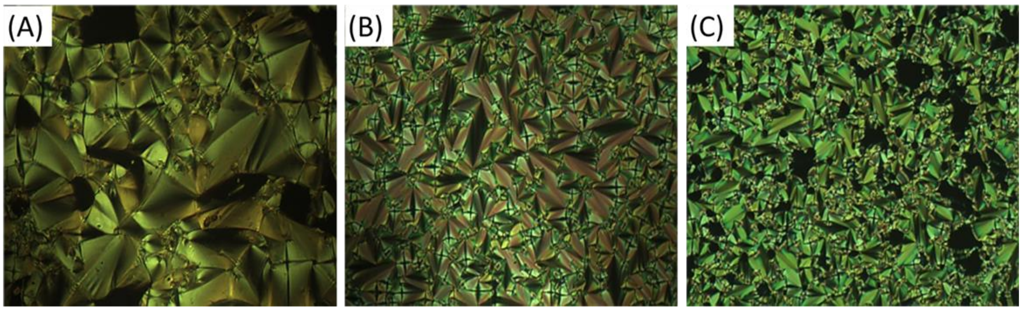

Fig. S4 Textures of *trans*-C_0-Chol observed by POM. (A) 179 °C upon first heating (obj x 10), (B) 173 °C upon first cooling (obj x 10), (C) 175 °C upon second heating (obj x 10).

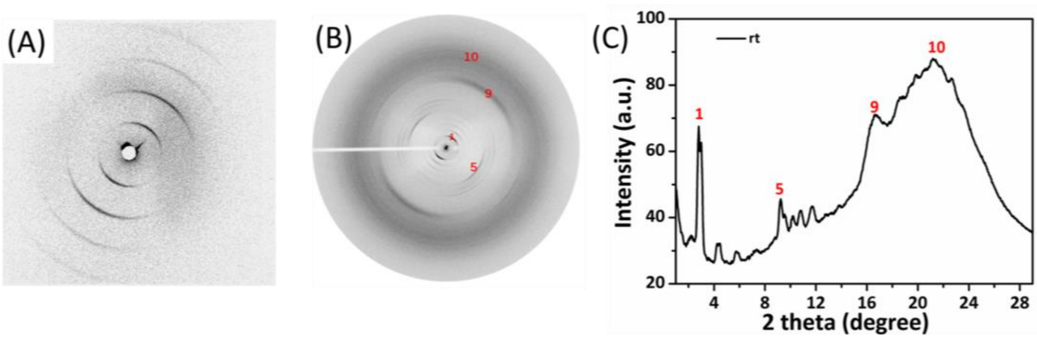

Fig. S5 Diffraction patterns of SAXS (A) and WAXS (B) of aligned sample of *trans*-C_5-Chol taken at 25°C. (C) is the intensity profile of WAXS signals in (B) as a function of diffraction angle 2θ (obtained by circular intensity integration).

Table S2. Diffraction angles and periodic distances (nm) obtained from SAXS and WAXS of *trans*-C_5-Chol

	peak	0	1	2	3	4	5	6	7	8	9	10
SAXS	2θ (°)	1.45	2.9	4.35	5.81	-	-	-	-	-	-	
	d (nm)	6.09	3.05	2.03	1.52	-	-	-	-	-	-	
WAXS	2θ (°)	-	2.81	4.46	5.74	7.35	9.23	10.21	10.79	11.67	16.68	21.19
	d (nm)	-	3.14	1.98	1.54	1.20	0.96	0.87	0.82	0.76	0.53	0.42

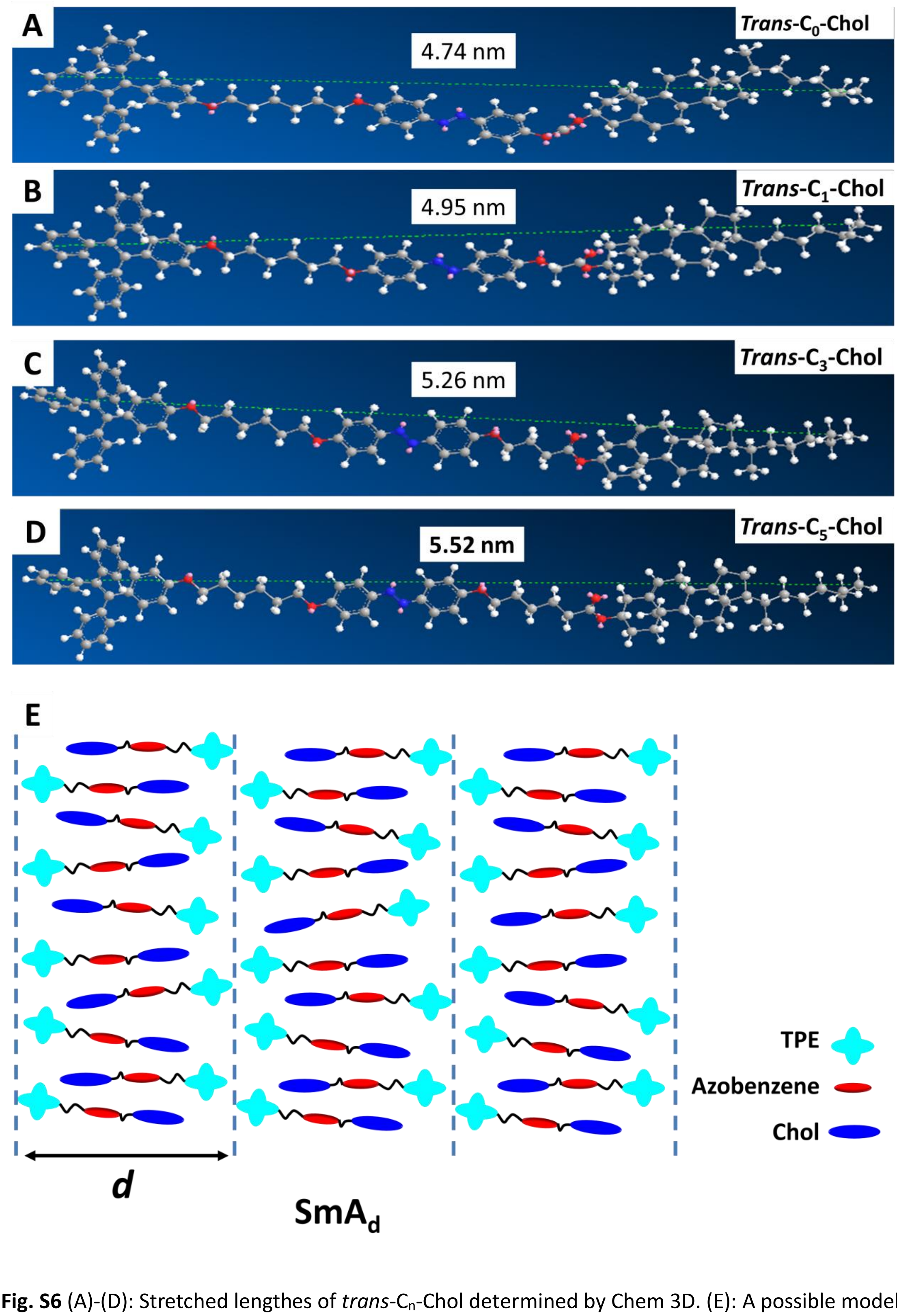

Fig. S6 (A)-(D): Stretched lengthes of *trans*-C_n-Chol determined by Chem 3D. (E): A possible model of molecular organization of SmA_d.

3. Gelation behavior

3.1 Gel ability

Table S3. Gelation properties of *trans*-C_n-Chol in organic solvents

Entry	Solvents	*trans*-C_5-Chol (CGC)[a] [mM]	*trans*-C_3-Chol (CGC) [mM]	*trans*-C_1-Chol (CGC) [mM]	*trans*-C_0-Chol (CGC) [mM]
1	DMSO	I	I	I	I
2	MeCN	I	I	I	I
3	DMF	G (29)	G (16)	P	P
4	Methanol	I	I	I	I
5	Ethanol	I	I	I	I
6	Acetone	G (48)	G (22)	P	P
7	THF	S	S	S	S
8	EA	G (46)	G (14)	P	P
9	DCM	S	S	S	S
10	Toluene	S	S	S	S
11	DCM/ EA = 1/2	G (36)	G (25)	P	P
12	THF/ EA = 1/2	P	P	P	P
13	DCM/ n-hexane = 1/2	P	P	P	P
14	Ethanol/ n-hexane	I	I	I	I

[a]The values in parentheses are critical gelation concentration (CGC, mM) at room temperature, I = insoluble when heated to 110 °C, G = stable gel at room temperature, P = precipitation when cooled from hot solution, S = soluble at room temperature.

3.2 Morphologies

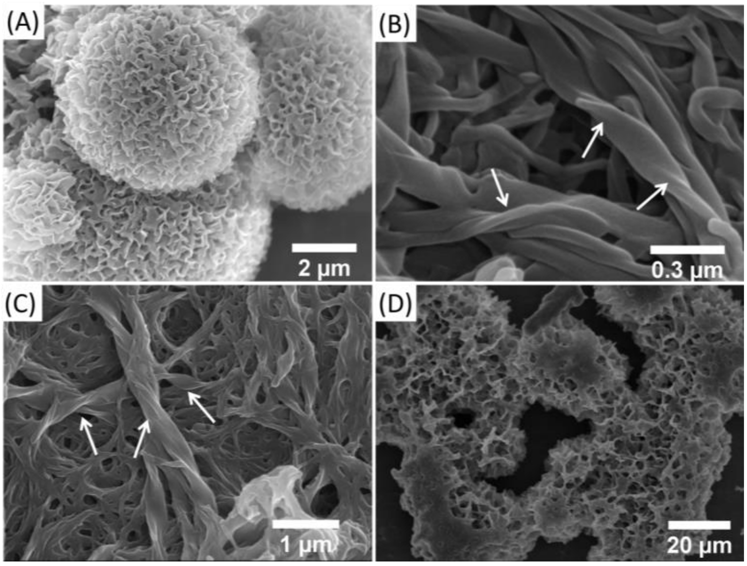

Fig. S7 SEM images of the gels of *trans*-C_3-Chol in (A) DMF, (B) acetone, (C) EA, and (D) DCM/EA (1/2, v/v).

3.3 Supramolecular chirality

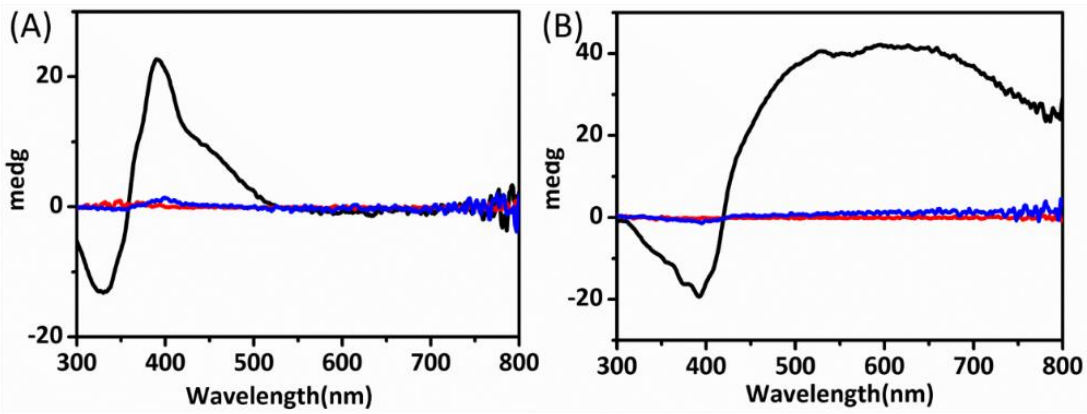

Fig. S8 CD spectra of the gels of *trans*-C_3-Chol (A) and *trans*-C_5-Chol (B) in DMF before (black) and after (blue) UV irradiation at 365 nm. Their CD spectra in THF solution are curves in red (Conc. = 0.1 mM).

3.4 Driving force of gelation

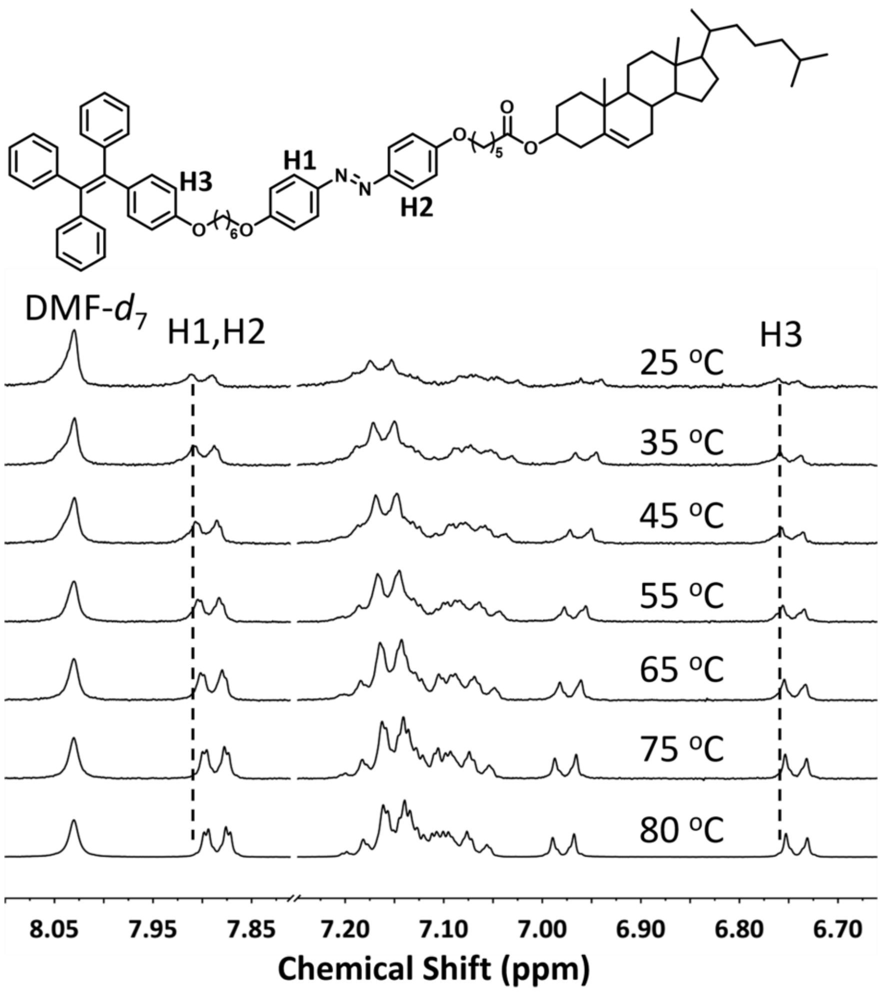

Fig. S9 Temperature-dependent ^{1}H NMR spectra (400 MHz) of *trans*-C_5-Chol gel in DMF-d_7.

4. AIE characteristics

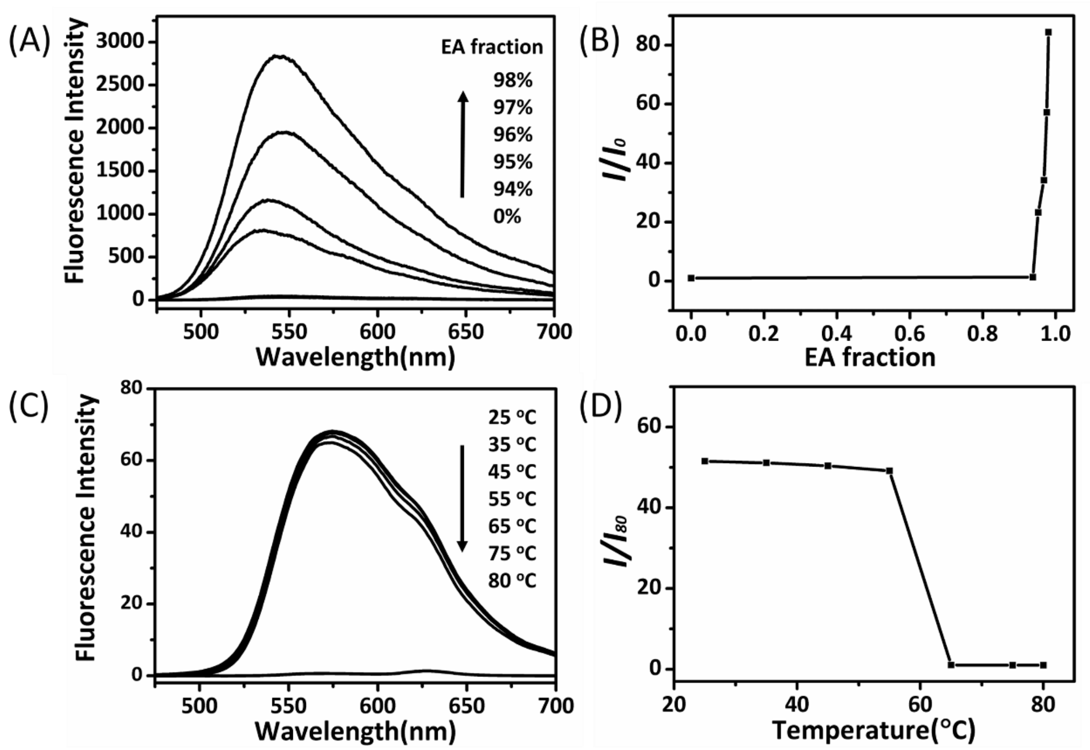

Fig. S10 (A) Fluorescence spectra of *trans*-C_3-chol in DCM/EA (conc. = 217 mM); (B) plots of I/I_0 of *trans*-C_3-Chol as a function of EA fraction in DCM/EA. I_0 = fluorescence peak intensity in DCM, I = fluorescence peak intensity in DCM/EA with different volume fractions; (C) temperature-dependent fluorescence spectra of *trans*-C_3-Chol gel in DMF (conc. = 20 mM); (D) plots of I/I_{80} of *trans*-C_3-Chol gel as a function of temperature from 25 to 80 °C. I_{80} = fluorescence peak intensity at 80 °C, I = fluorescence peak intensity at other temperature (25, 35, 45, 55, 65, and 75 °C). λ_{Ex} = 310 nm.

5. Photo-responsiveness

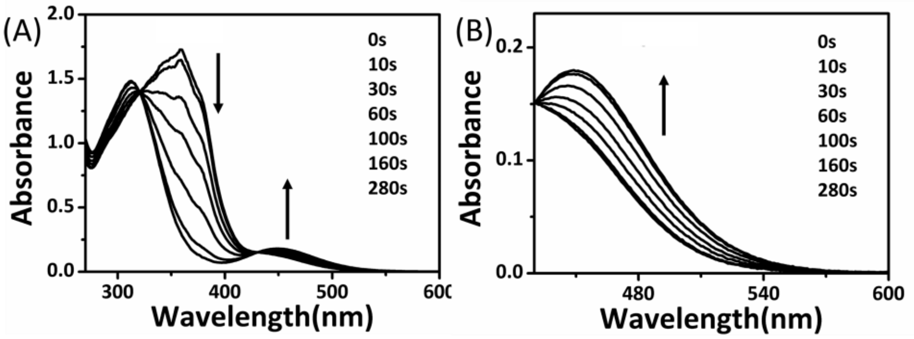

Fig. S11 (A) UV-Vis spectra of *trans*-C_3-Chol in DMF (conc. 0.084 mM) with different irradiation time of UV light; (B) enlarged 430-600 nm of in (A) (0.25 mW/cm^2, 365 nm).

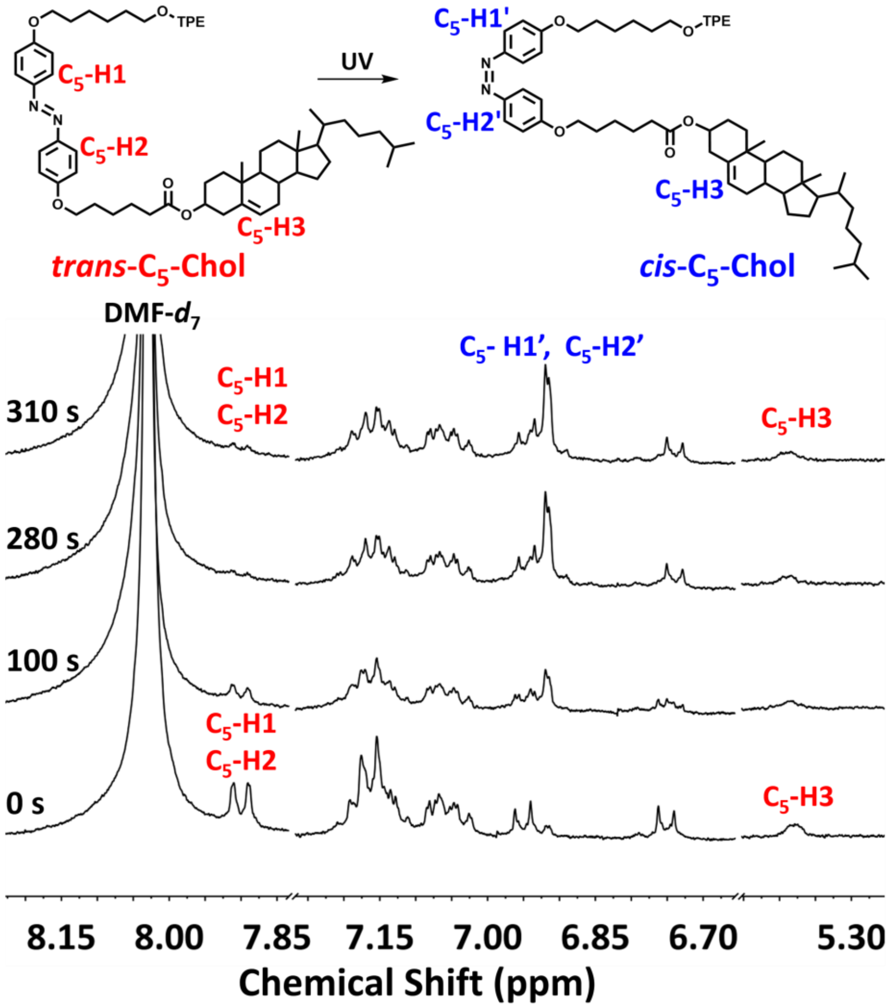

Fig. S12 ^{1}H NMR (400 MHz) of *trans*-C_5-Chol gel in DMF-d_7 (c = 0.18 mM) under UV irradiation at 365 nm as a function of irradiation time (UV intensity: 0.25 mW/cm^2).

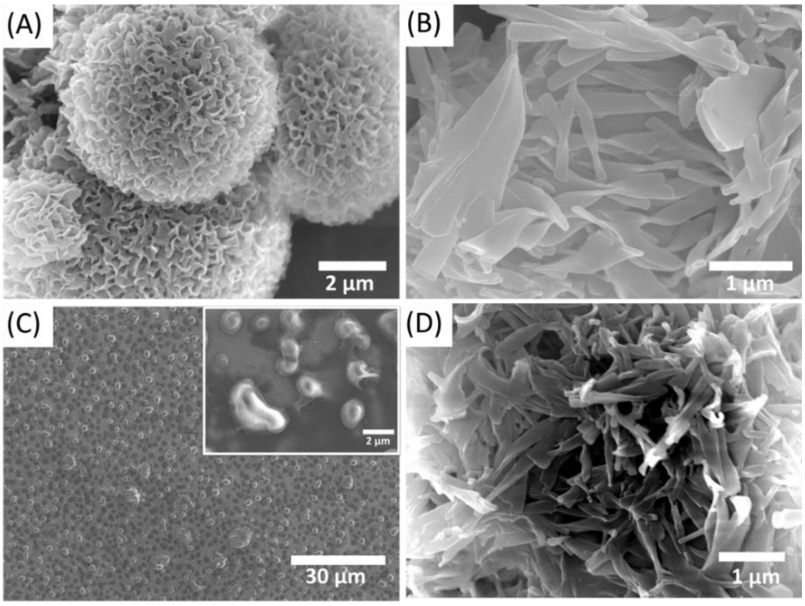

Fig. S13 (A) and (B): SEM images of gels of (A) *trans*-C_3-Chol, (B) *trans*-C_5-Chol in DMF. (C) and (D): SEM images of the residues collected from collapsed gels of (C) *trans*-C_3-Chol, (D) *trans*-C_5-Chol after UV irradiation for 15 min (90 mW/cm^2, 365 nm).

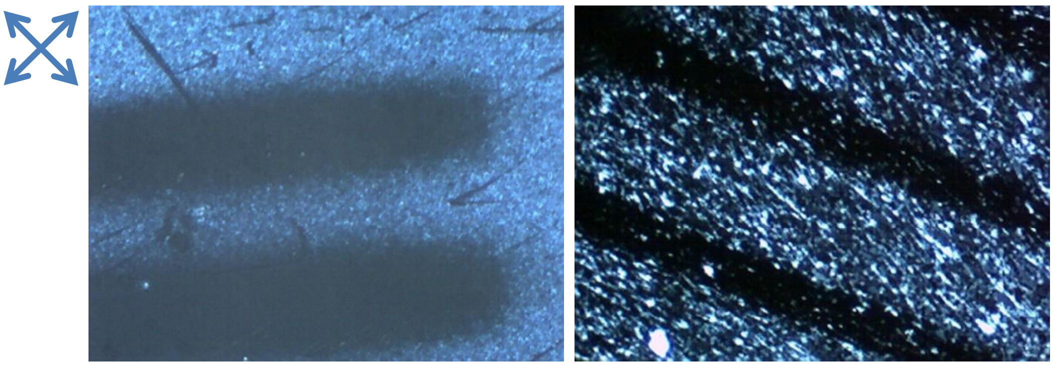

Fig. S14 (A) POM photograph of *trans*-C_0-Chol film after UV irradiation under the mask (width of strip: 100 µm; distance between two stripes: 200 µm). (B) POM photograph of *trans*-C_1-Chol film after UV irradiation under the mask (width of strip: 50 µm; distance between two stripes: 200 µm). For both sample, UV wavelength: 365 nm; UV intensity: 70 mW/cm^{-2}; duration: 60 min.

6. MS, ^{1}H and ^{13}C NMR spectra

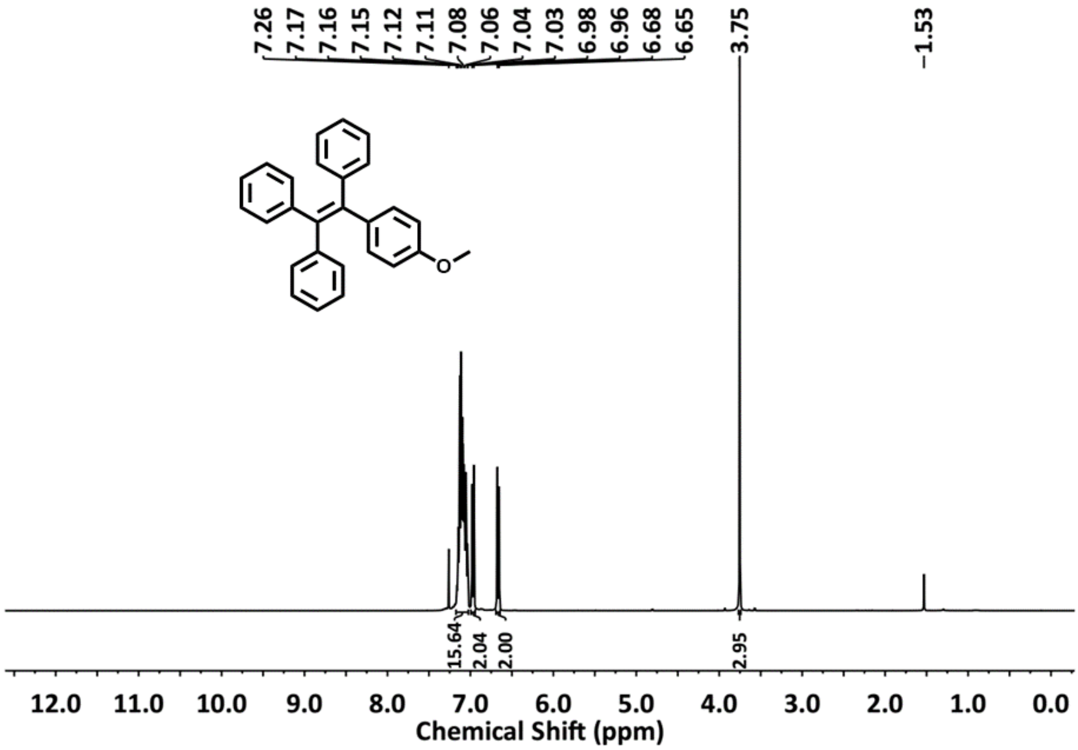

Fig. S15 ^{1}H NMR spectra of **TPE-OMe** in $CDCl_3$ (400 MHz).

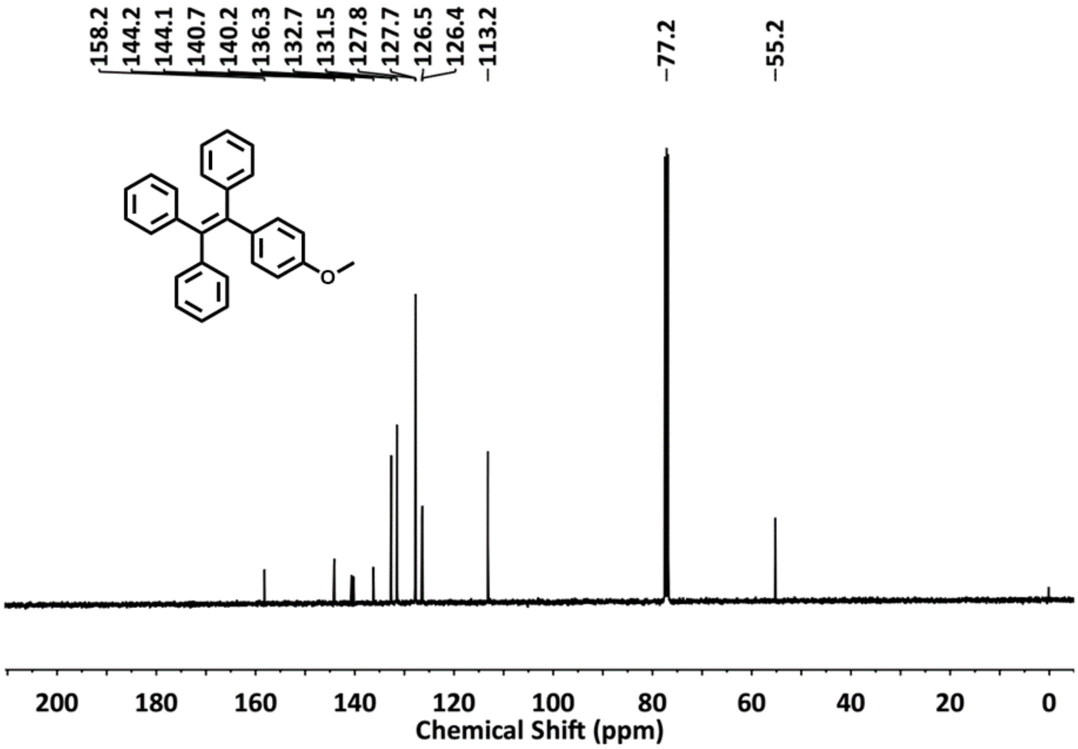

Fig. S16 ^{13}C NMR spectra of **TPE-OMe** in $CDCl_3$ (100 MHz).

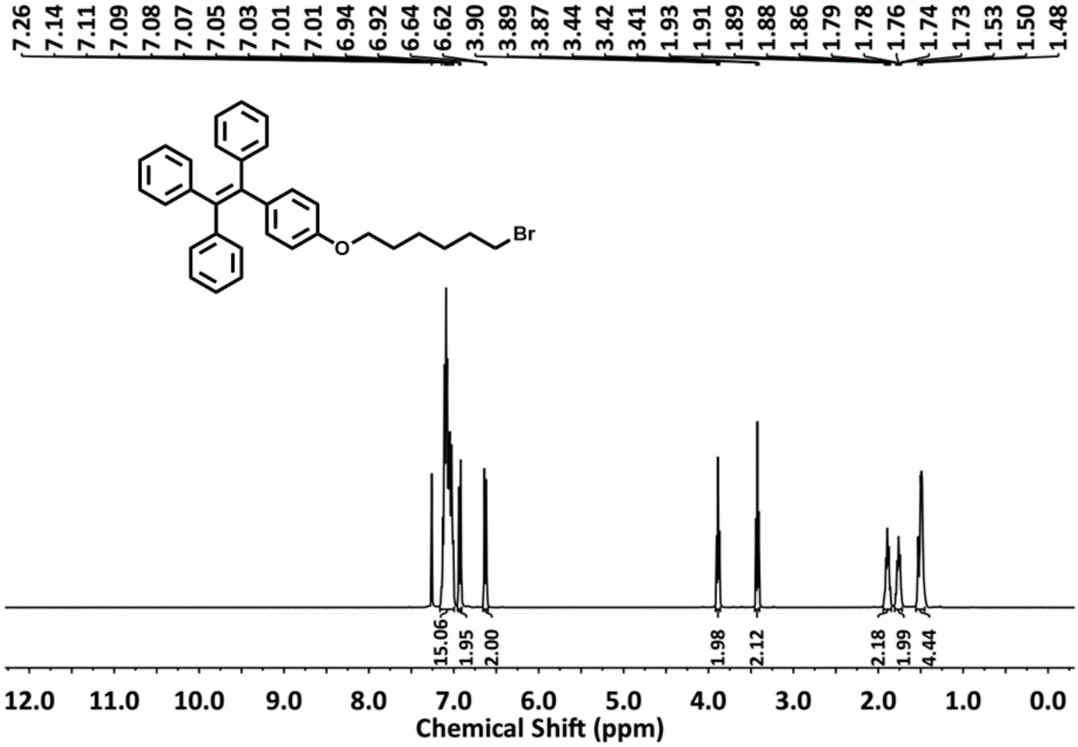

Fig. S17 ^{1}H NMR spectra of **TPE-C$_6$-Br** in $CDCl_3$ (400 MHz).

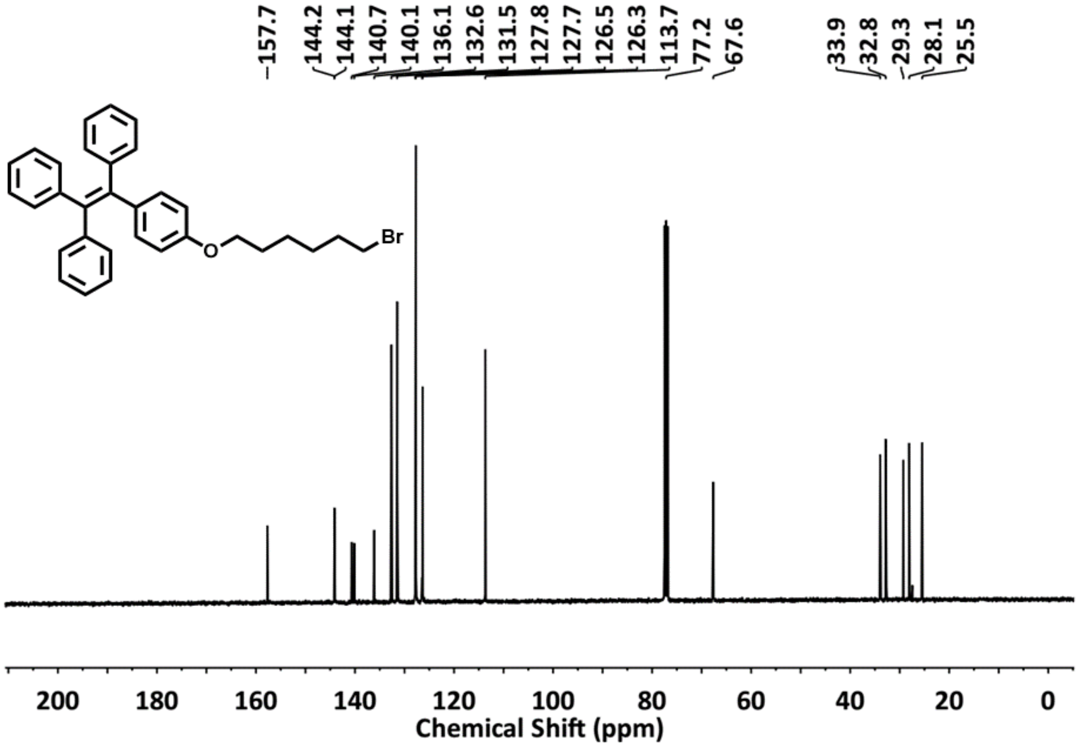

Fig. S18 ^{13}C NMR spectra of **TPE-C$_6$-Br** in $CDCl_3$ (100 MHz).

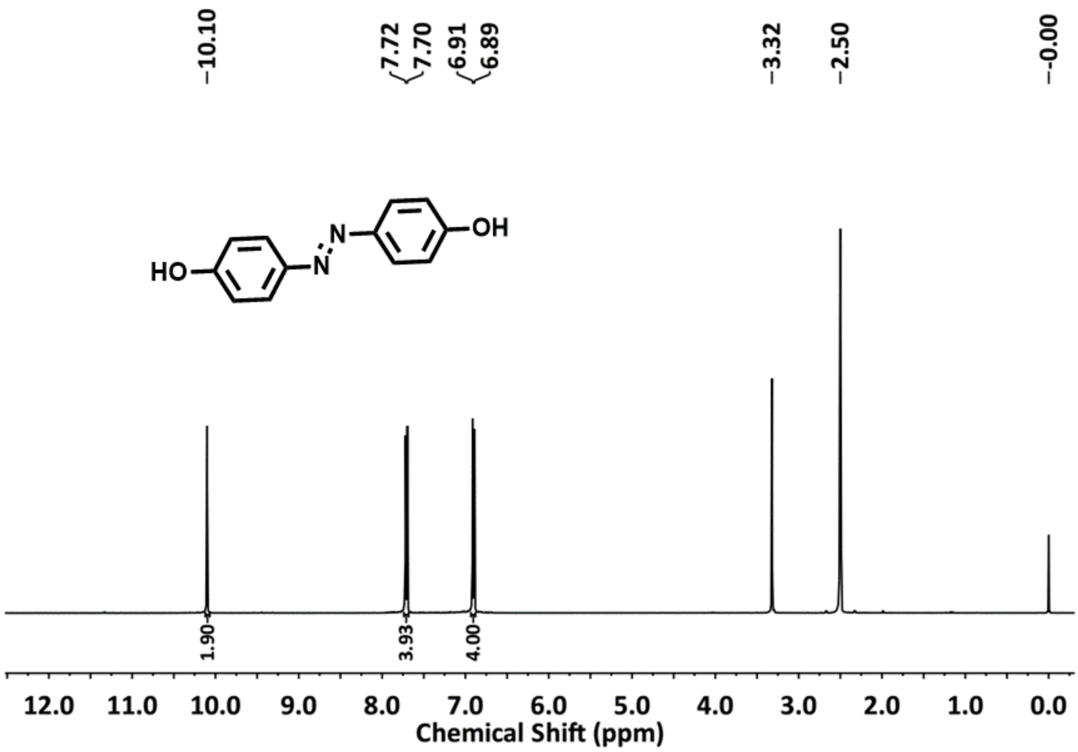

Fig. S19 ^{1}H NMR spectra of ***trans*-azophenol** in DMSO-d_6 (400 MHz).

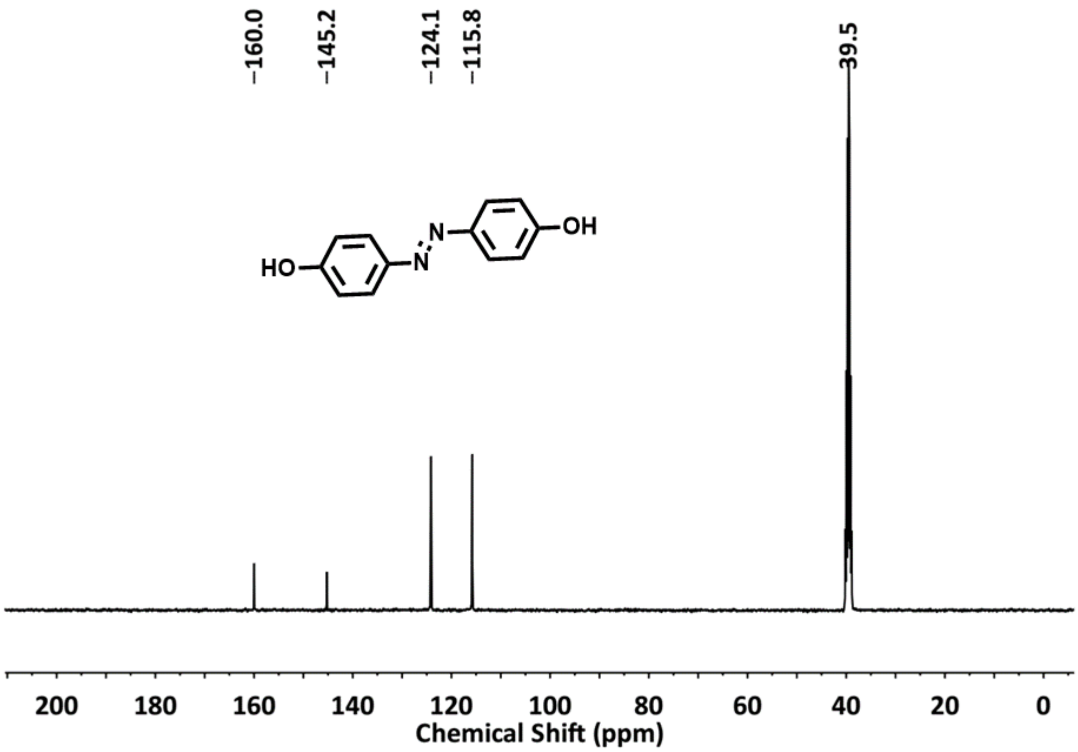

Fig. S20 ^{13}C NMR spectra of ***trans*-azophenol** in DMSO-d_6 (100 MHz).

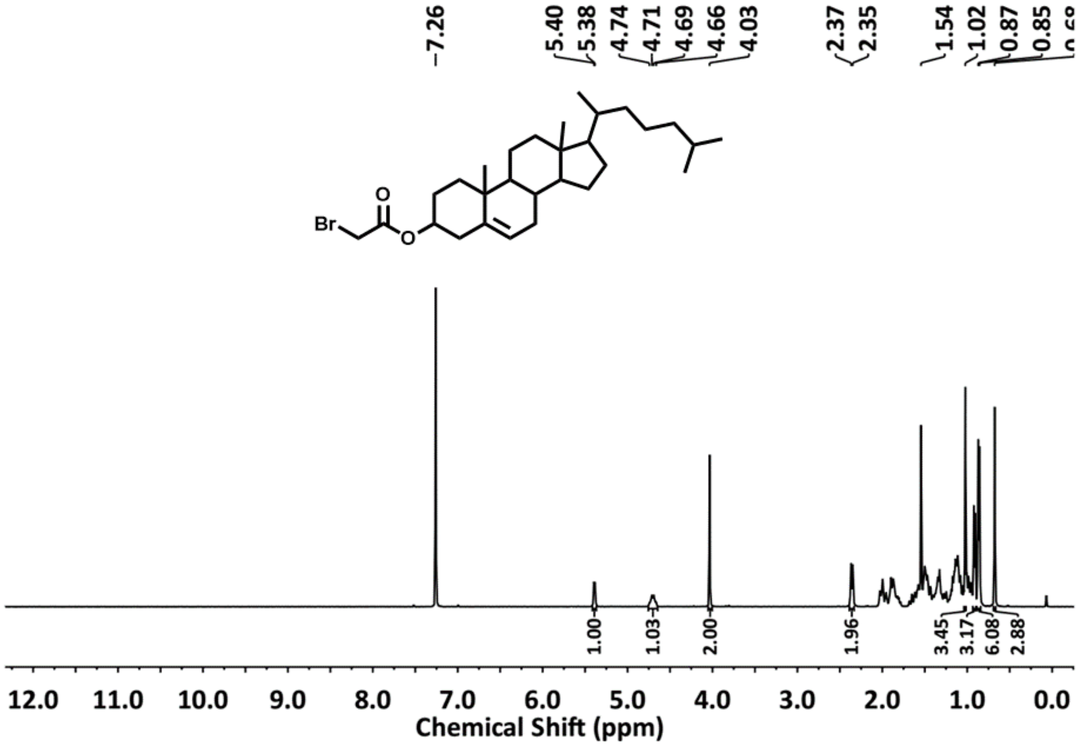

Fig. S21 ^{1}H NMR spectra of **Br-C_1-Chol** in $CDCl_3$ (400 MHz).

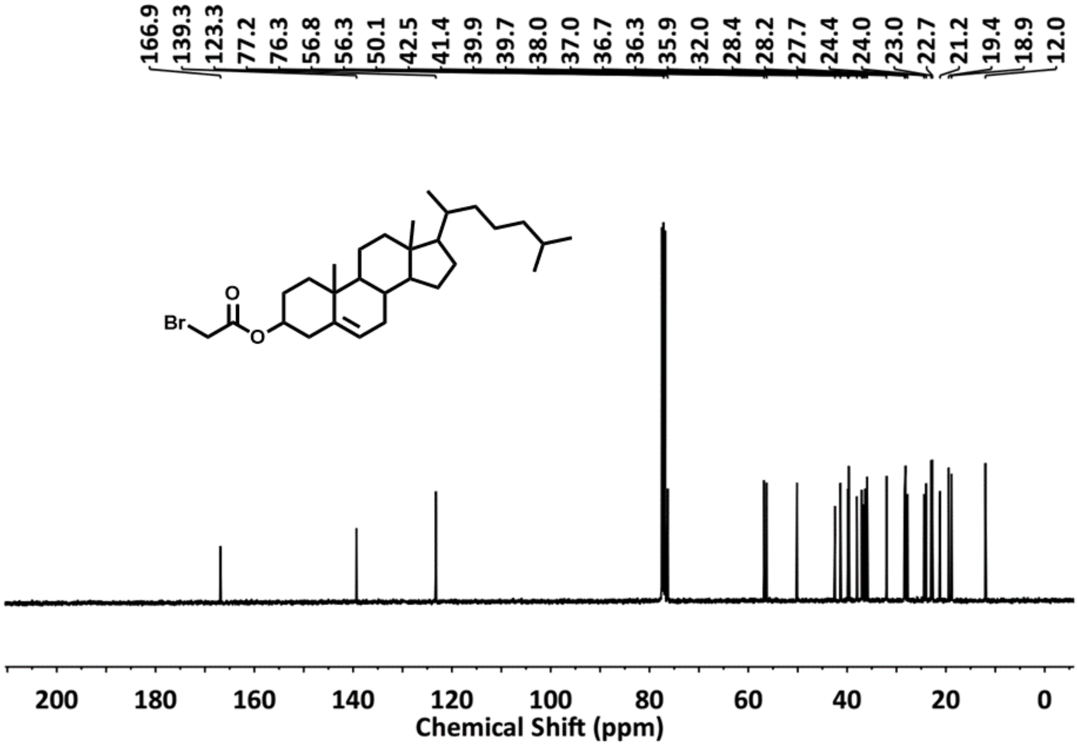

Fig. S22 ^{13}C NMR spectra of **Br-C_1-Chol** in $CDCl_3$ (100 MHz).

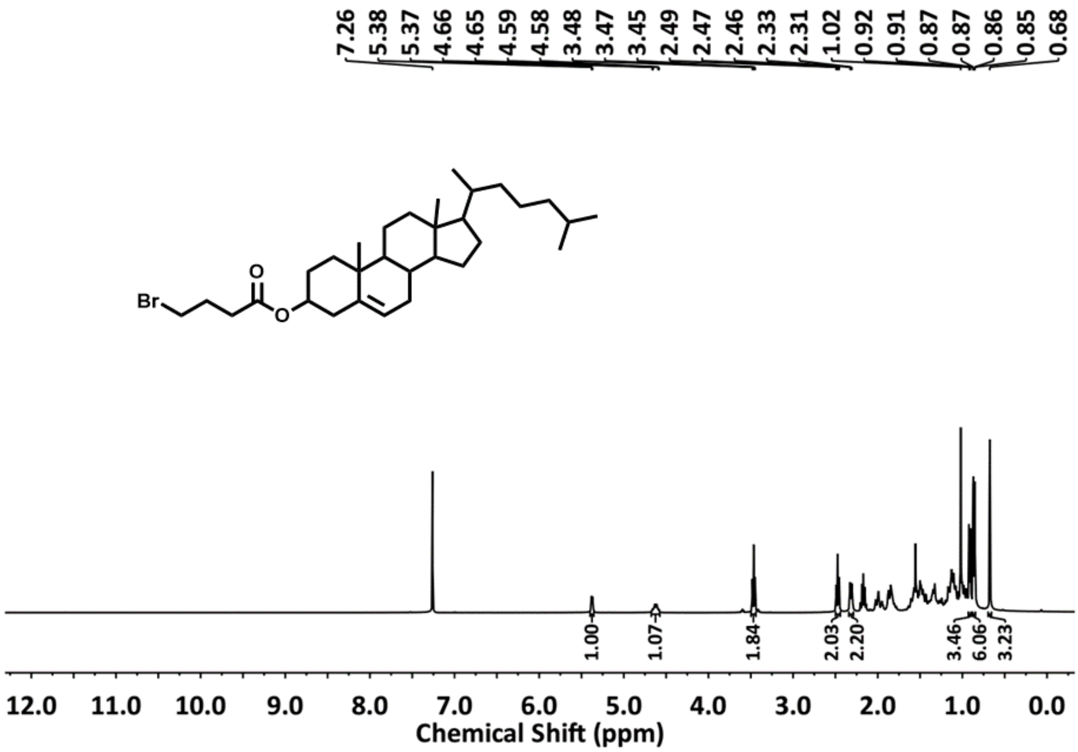

Fig. S23 ^{1}H NMR spectra of **Br-C$_3$-Chol** in $CDCl_3$ (400 MHz).

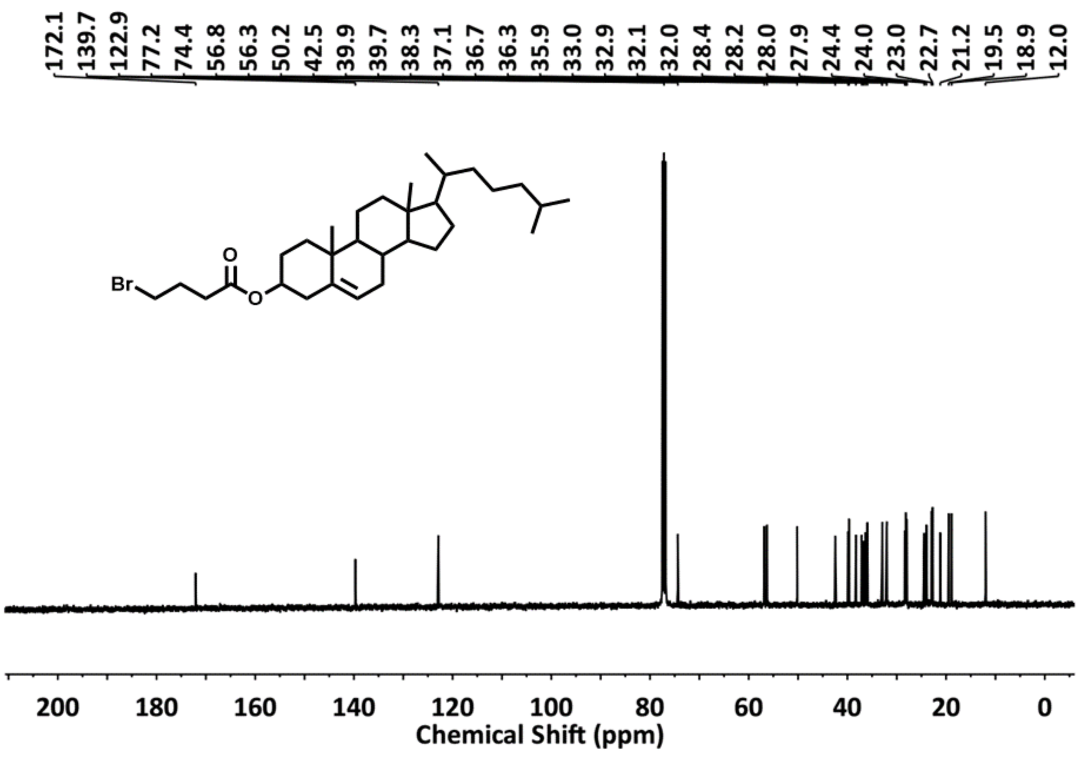

Fig. S24 ^{13}C NMR spectra of **Br-C$_3$-Chol** in $CDCl_3$ (100 MHz).

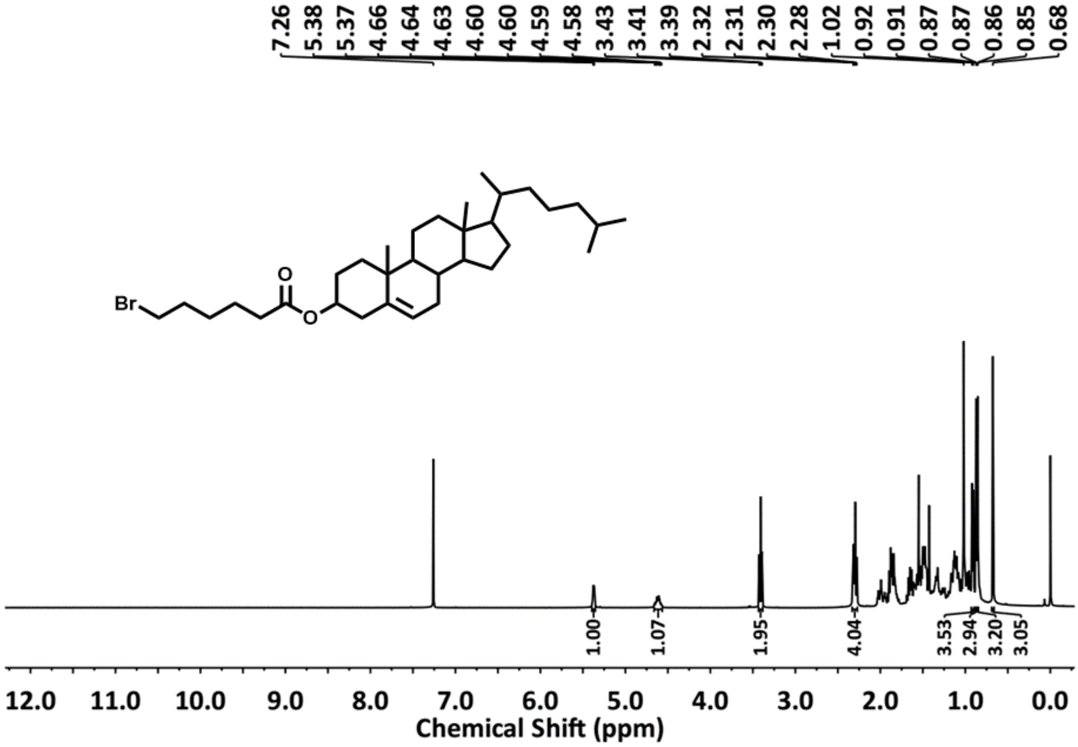

Fig. S25 ^{1}H NMR spectra of **Br-C_5-Chol** in $CDCl_3$ (400 MHz).

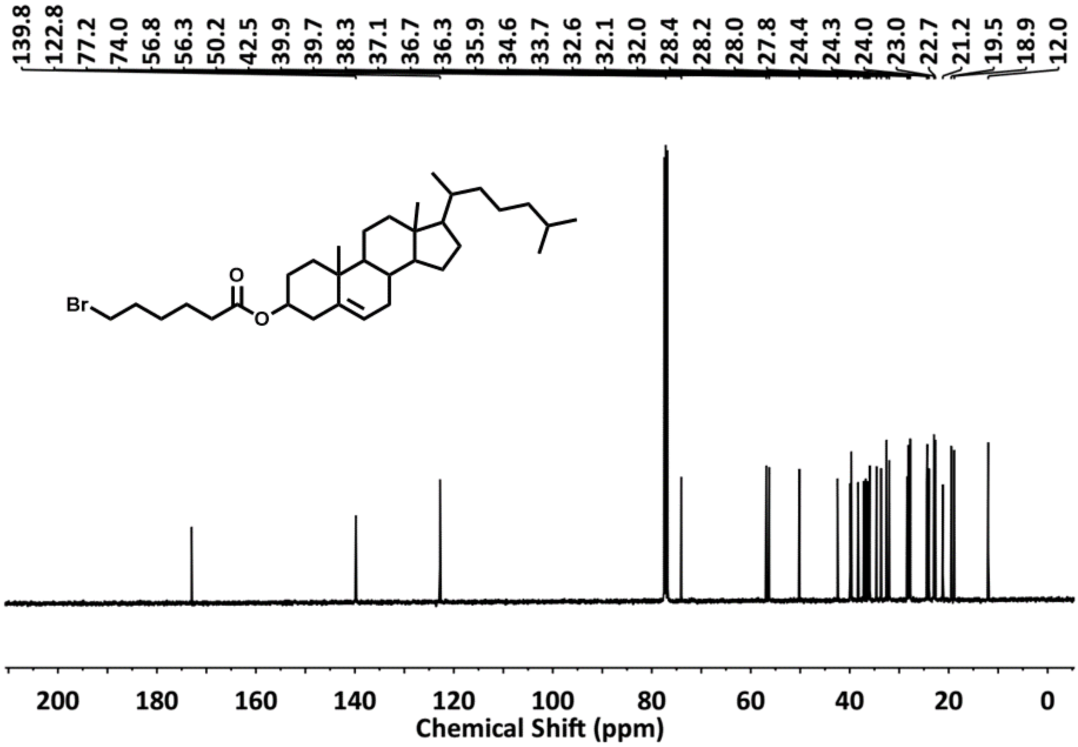

Fig. S26 ^{13}C NMR spectra of **Br-C_5-Chol** in $CDCl_3$ (100 MHz).

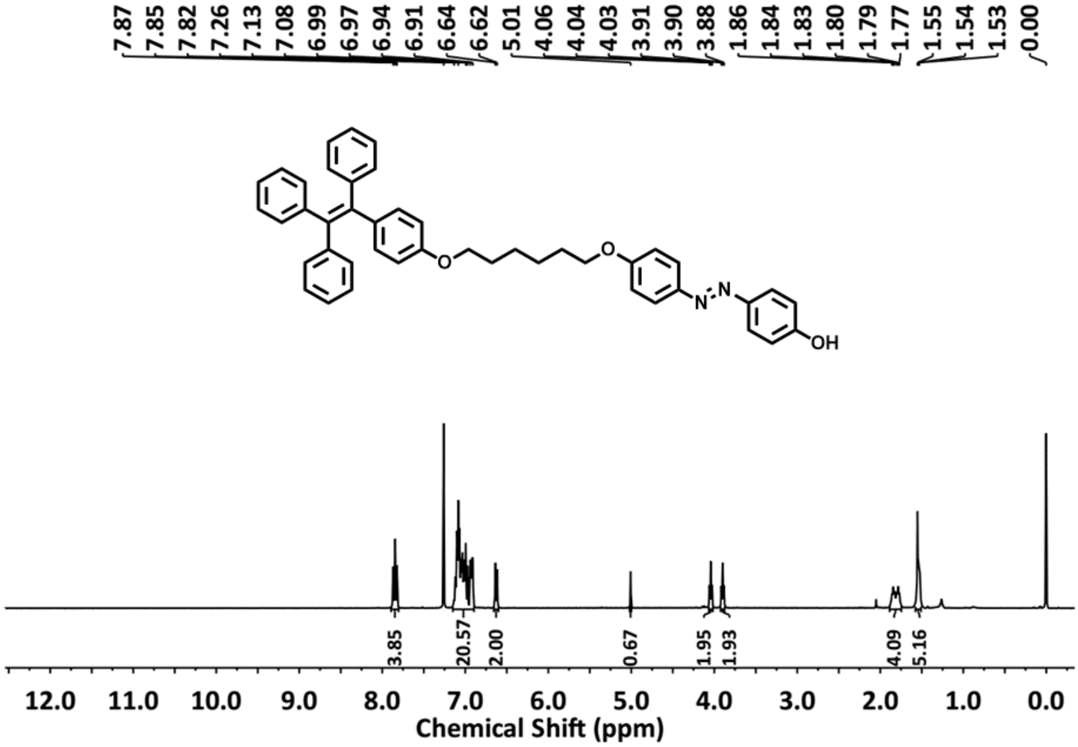

Fig. S27 ^{1}H NMR spectra of ***trans*-TPE-C$_6$-azohenol** in $CDCl_3$ (400 MHz).

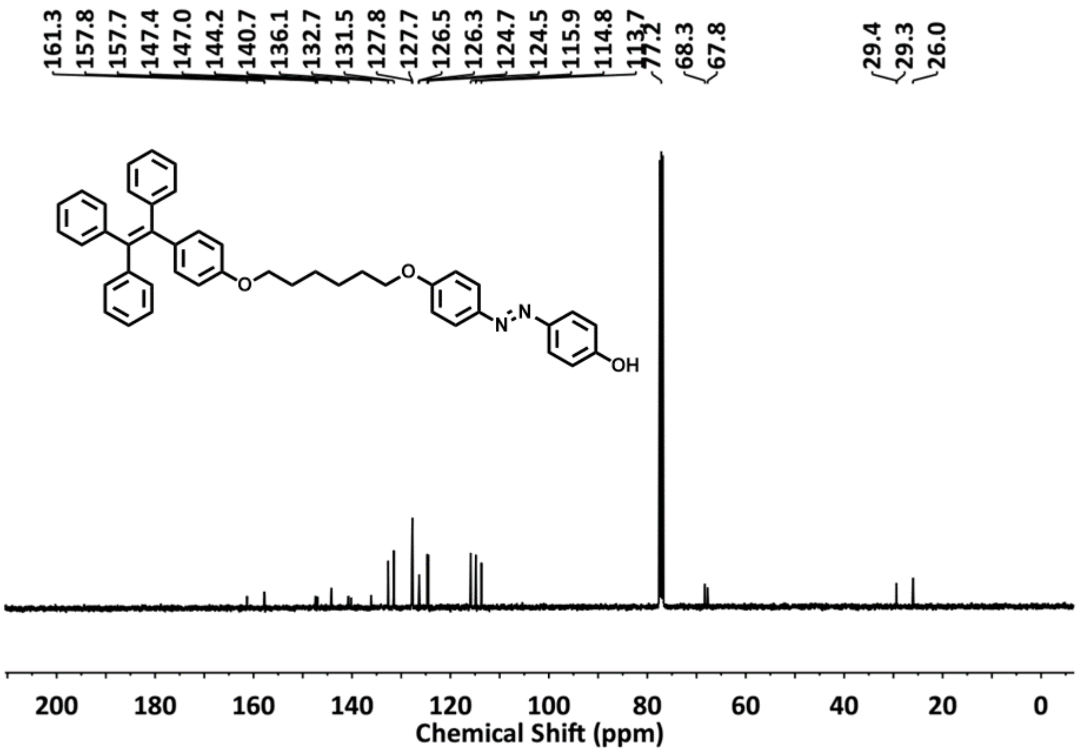

Fig. S28 ^{13}C NMR spectra of ***trans*-TPE-C$_6$-azohenol** in $CDCl_3$ (100 MHz).

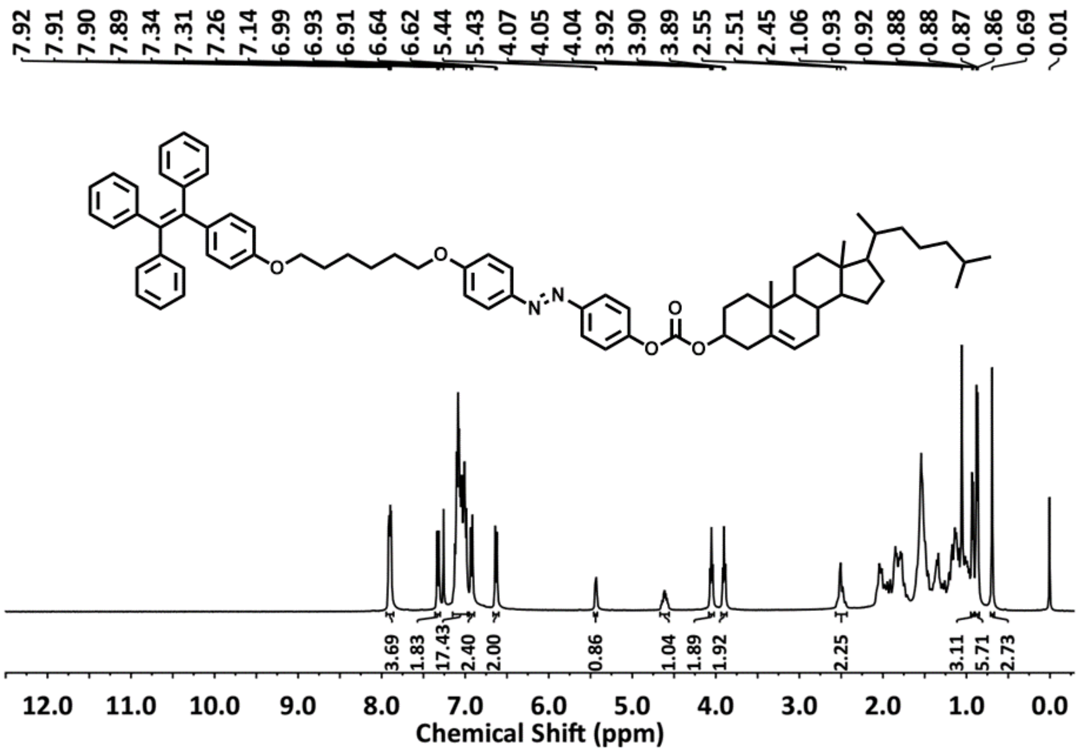

Fig. S29 ^{1}H NMR spectra of ***trans*-C$_0$-Chol** in $CDCl_3$ (400 MHz).

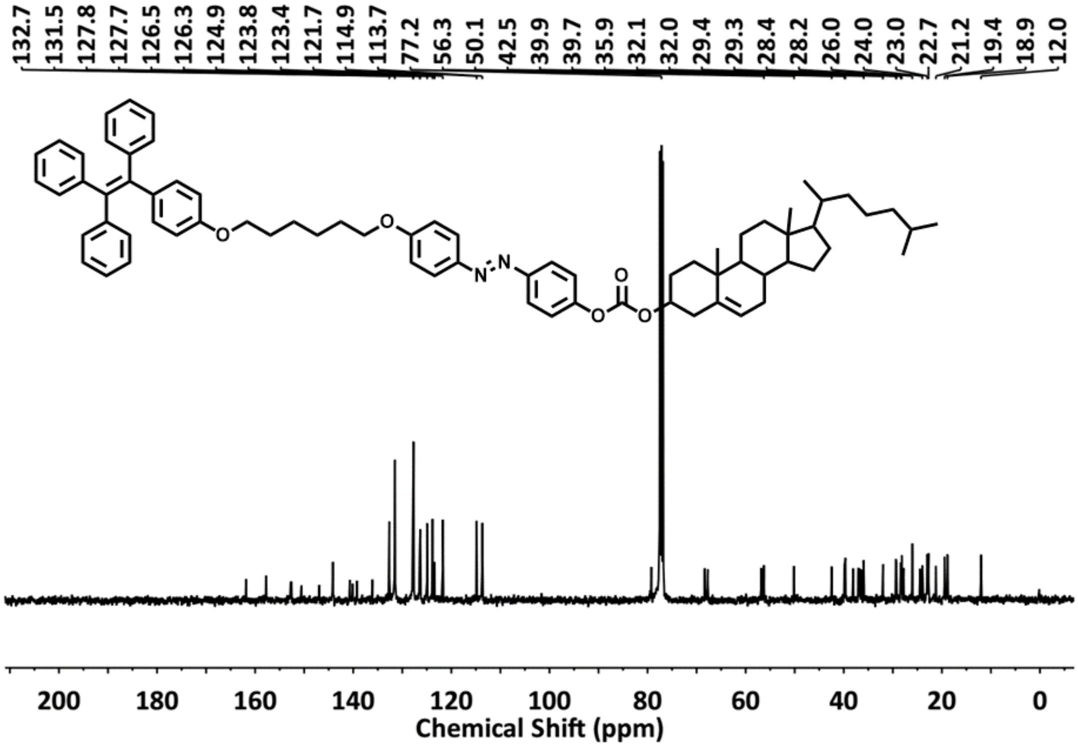

Fig. S30 ^{13}C NMR spectra of ***trans*-C$_0$-Chol** in $CDCl_3$ (100 MHz).

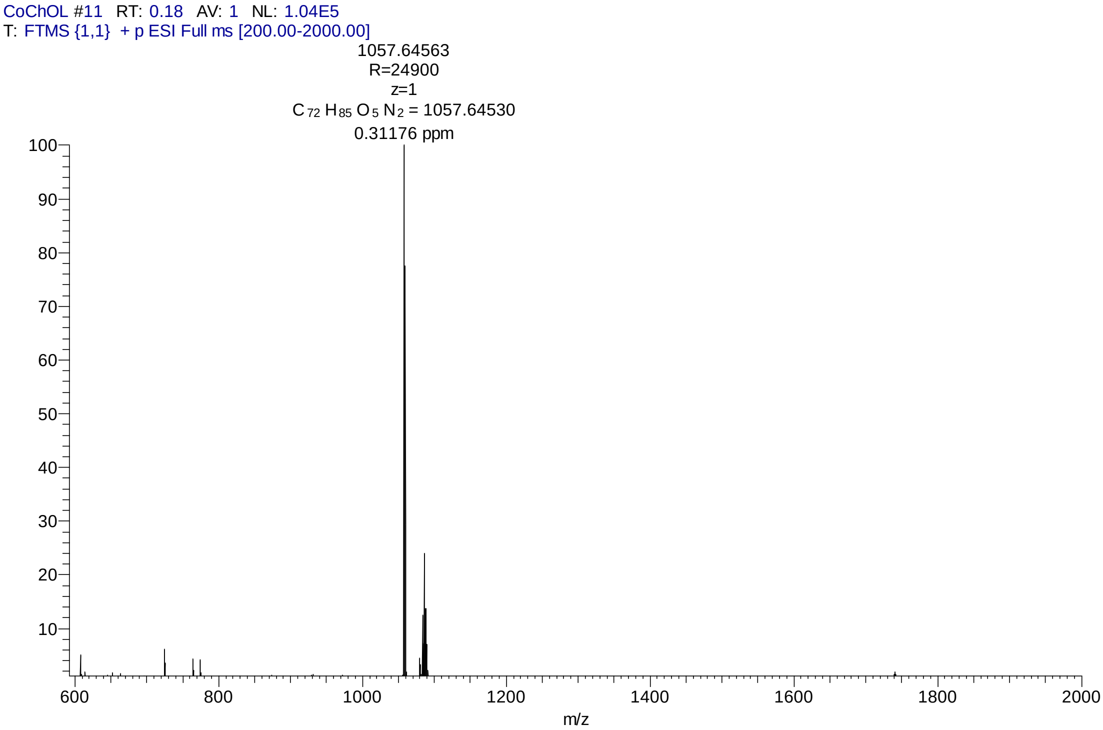

Fig. S31 ESI-HRMS (+) of ***trans*-C$_0$-Chol**

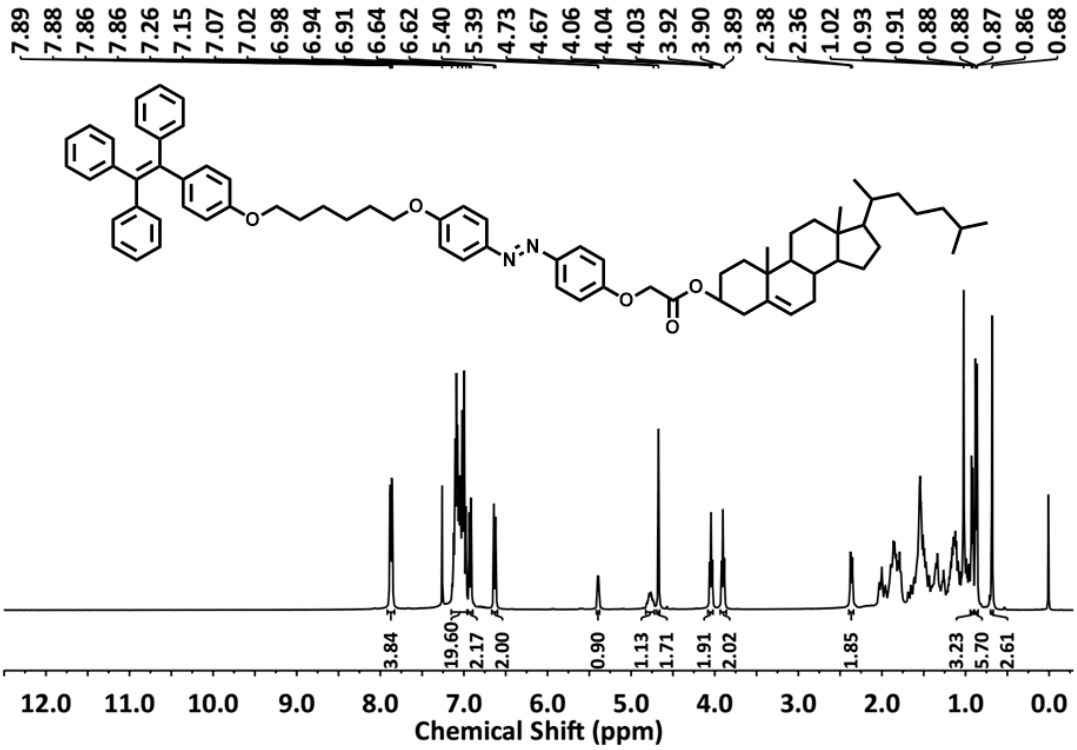

Fig. S32 ^{1}H NMR spectra of ***trans*-C$_1$-Chol** in $CDCl_3$ (400 MHz).

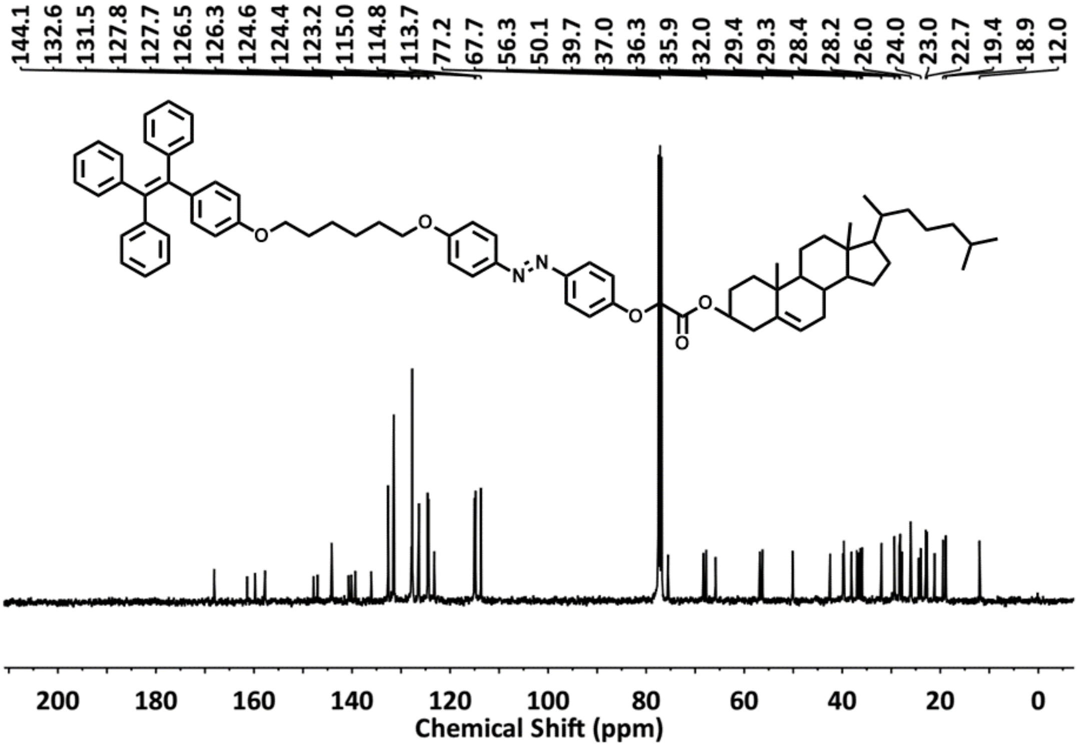

Fig. S33 ^{13}C NMR spectra of ***trans*-C$_1$-Chol** in $CDCl_3$ (100 MHz).

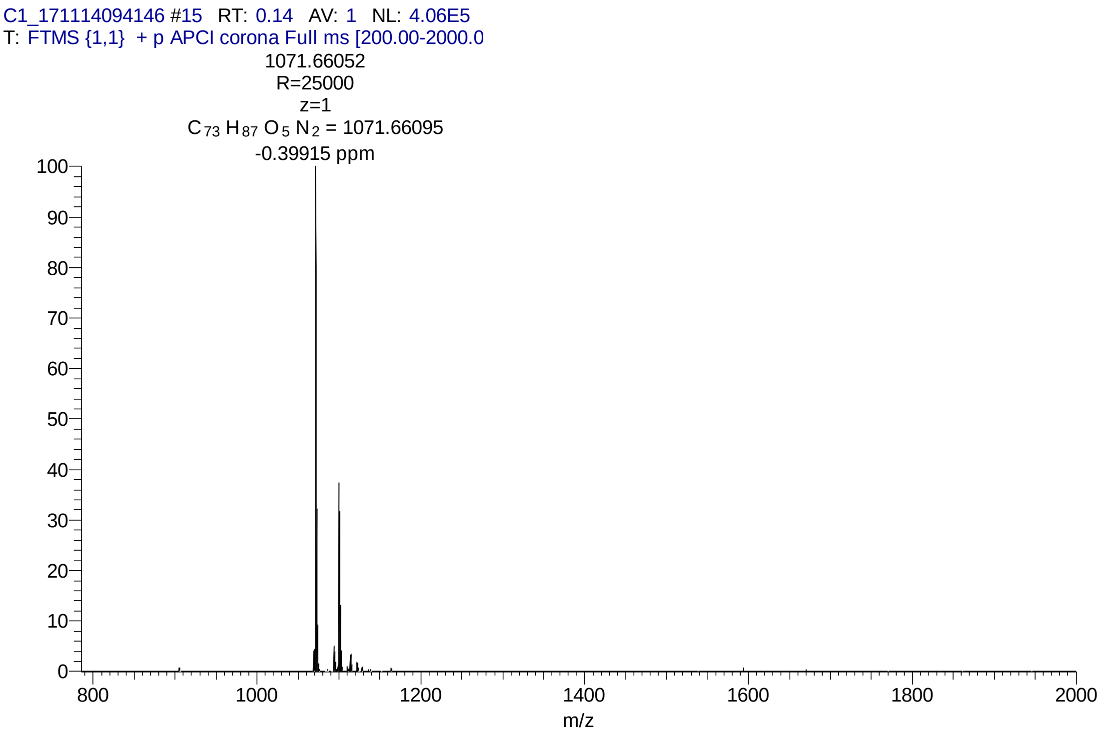

Fig. S34 ESI-HRMS (+) of ***trans*-C$_1$-Chol**

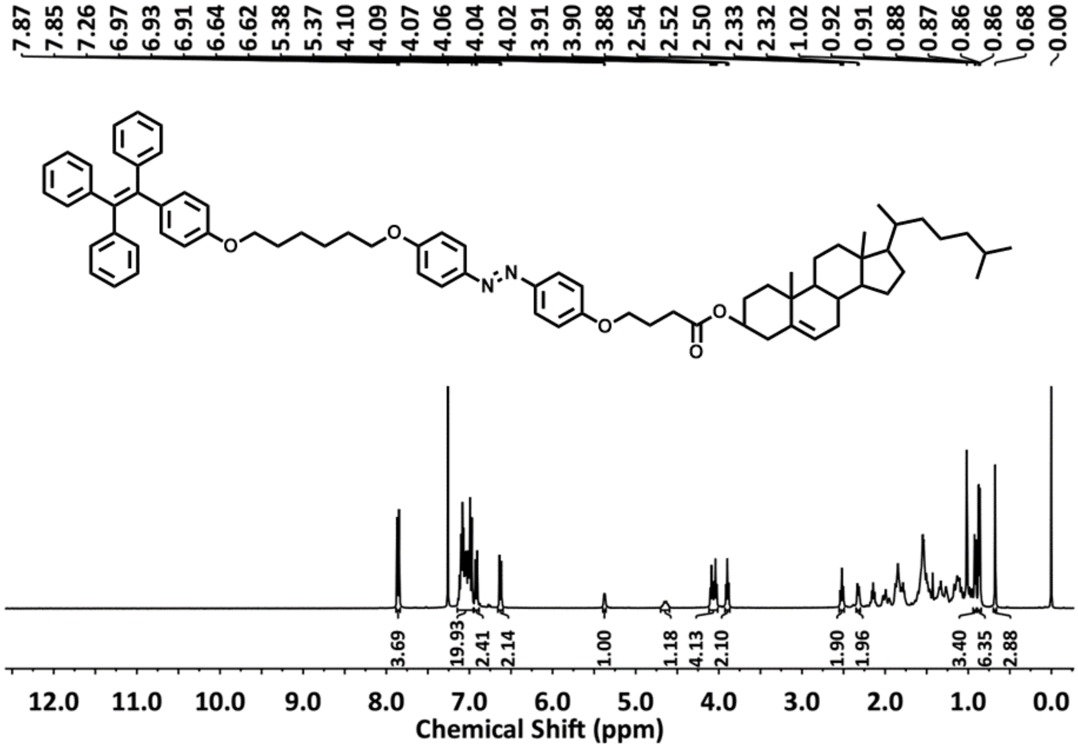

Fig. S35 ^{1}H NMR spectra of ***trans*-C$_3$-Chol** in $CDCl_3$ (400 MHz).

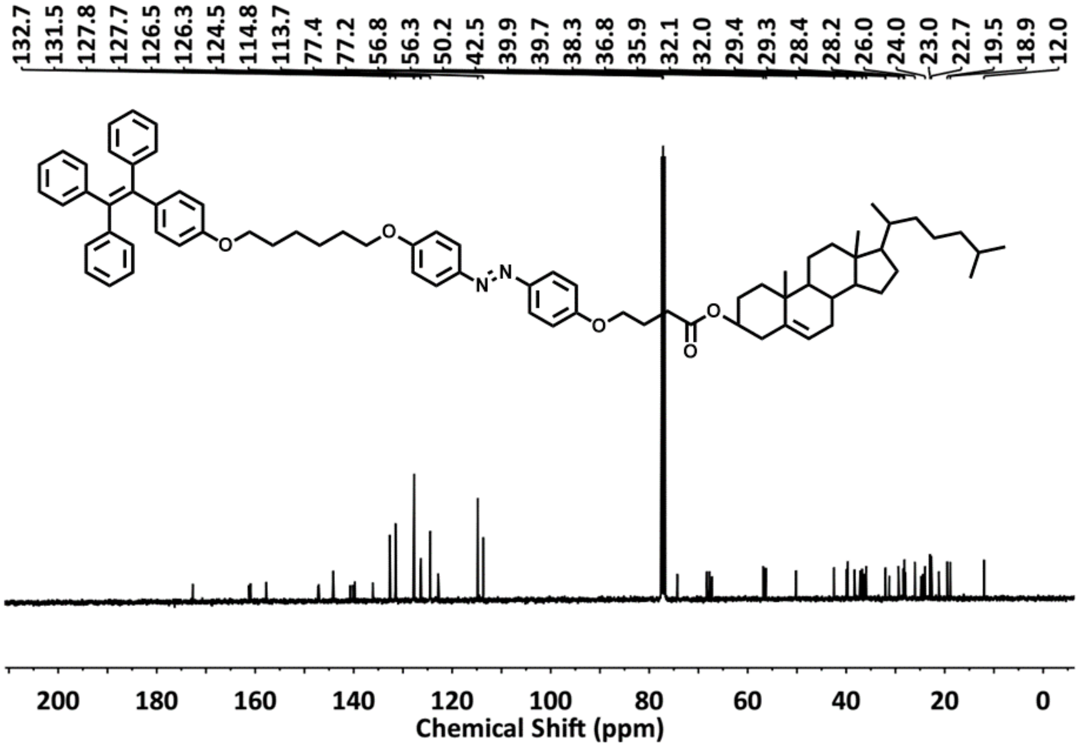

Fig. S36 ^{13}C NMR spectra of ***trans*-C$_3$-Chol** in $CDCl_3$ (100 MHz).

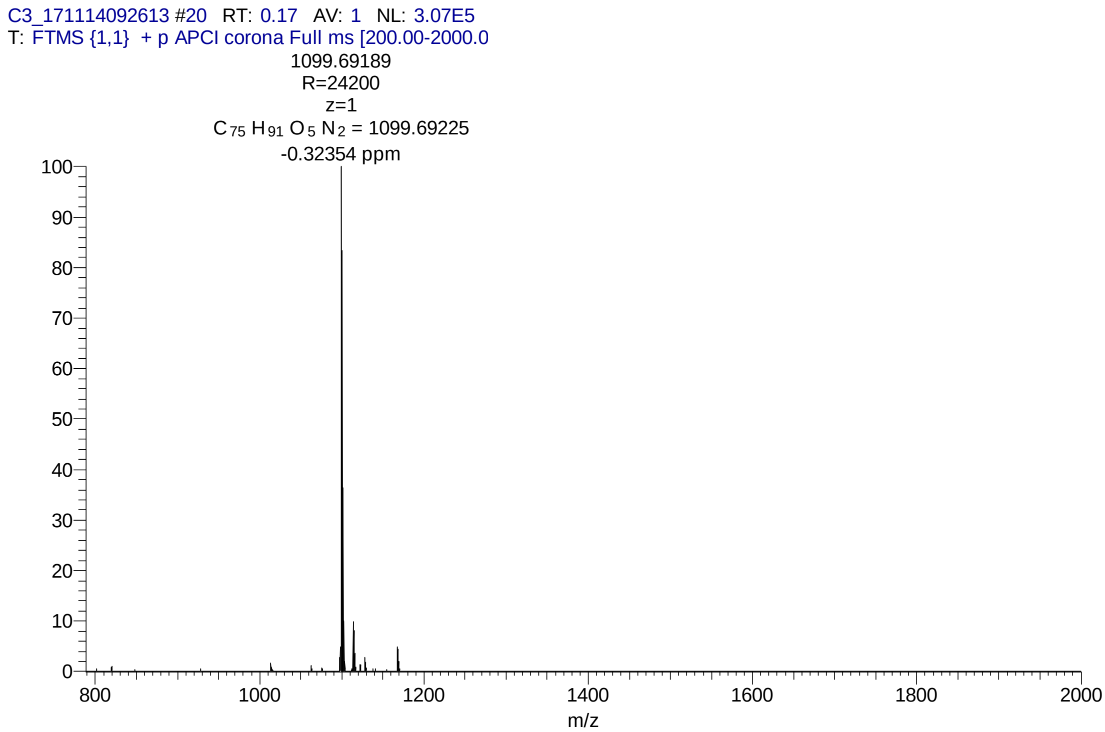

Fig. S37 ESI-HRMS (+) of ***trans*-C$_3$-Chol**

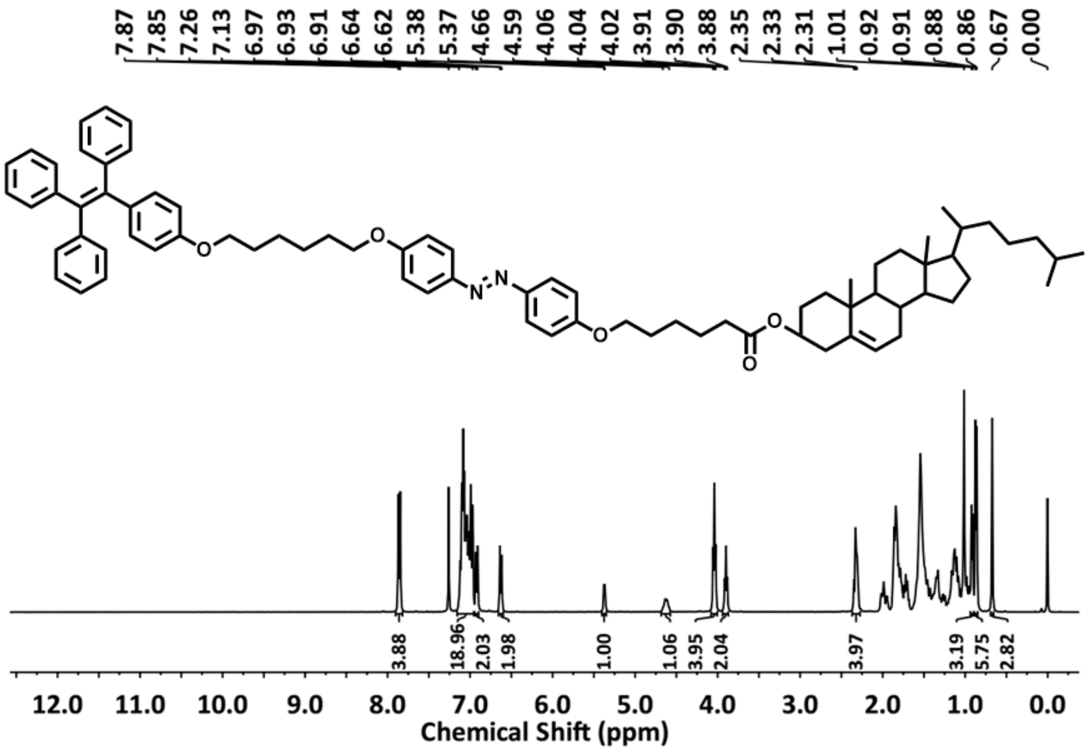

Fig. S38 [1]H NMR spectra of ***trans*-C$_5$-Chol** in CDCl$_3$ (400 MHz).

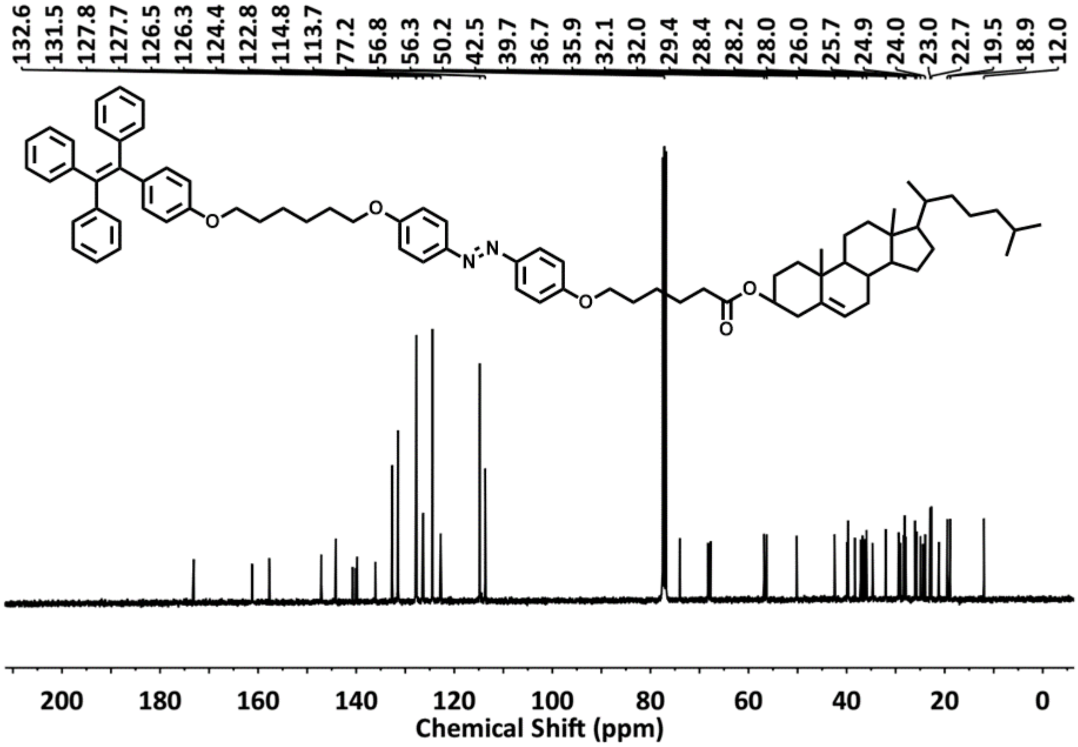

Fig. S39 ^{13}C NMR spectra of ***trans*-C_5-Chol** in $CDCl_3$ (100 MHz).

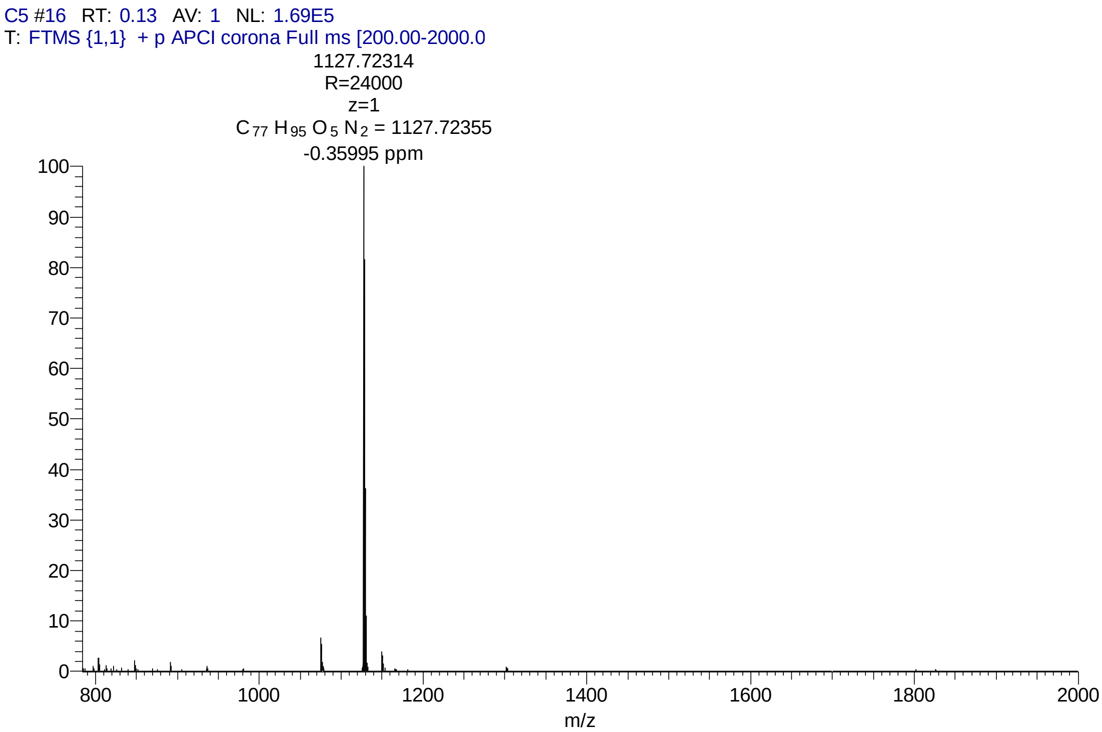

Fig. S40 ESI-HRMS (+) of ***trans*-C_5-Chol**